

Preparation, Characterization, and Polymerization of Chromium Complexes-Grafted Al/SBA-15 and Ti/SBA-15 Nanosupports

Ebrahim Ahmadi,¹ Zahra Mohamadnia,² Asemeh Mashhadi-Malekzadeh,¹
Zahra Hamdi,¹ Fatemeh Saghatchi¹

¹Polymer Synthesis Laboratory, Chemistry Department, Zanjan University, Zanjan, Iran

²Department of Chemical Engineering, Zanjan University, Zanjan, Iran

Correspondence to: E. Ahmadi (E-mail: ahmadi@znu.ac.ir)

ABSTRACT: Ethylene polymerization catalysts have been prepared by grafting chromium (III) nitrate onto Al/SBA-15 and Ti/SBA-15 mesoporous materials. A combination of XRD, nitrogen adsorption, TEM, and inductively coupled plasma-atomic emission spectroscopy (ICP-AES), were used to characterize the catalysts. Polymerization activity of Cr/SBA-15 catalyst is significantly improved by Al or Ti insertion to the supports. Particularly, the chromium catalyst prepared with Ti/SBA-15 support is more active than Al/SBA-15 catalyst. © 2012 Wiley Periodicals, Inc. *J. Appl. Polym. Sci.* 128: 4245–4252, 2013

KEYWORDS: catalysts; supports; polyethylene

Received 1 June 2011; accepted 13 July 2012; published online 22 October 2012

DOI: 10.1002/app.38353

INTRODUCTION

Commercial linear polyethylene, the most commonly used type of plastic, was born more than half a century ago with the accidental discovery at Phillips Petroleum Company that chromium oxide supported on silica can polymerize α -olefins.¹ The same catalyst system, modified and evolved, is used even today by dozens of companies throughout the world, and it accounts for a large share of the world's high-density polyethylene (HDPE) supply, as well as some low-density polymers. The catalyst is now more active and has been tailored in numerous ways for many specialized modern applications.

Broadly speaking, the Phillips catalyst consists of hexavalent chromium supported on a high-surface-area, wide-pore oxide carrier, such as silica, alumina, titania, aluminophosphates, or combinations thereof. Usually, the carrier is mainly composed of silica. To make the catalyst, the carrier is impregnated with a chromium compound followed by calcination in dry air or oxygen to "activate" the catalyst.^{2–4} During this activation, chromium becomes oxidized to Cr(VI), which reacts with surface hydroxyl groups to become anchored and monodispersed. This process stabilizes the Cr(VI) against thermal decomposition.

Nowadays, it is well known that activity of Phillips catalysts is very sensitive toward preparation methods (chromium anchorage and subsequent activation) and support physicochemical properties, both playing an important role on the resulting properties of the produced polyethylene.^{5–10}

SBA-15, which was synthesized by Zhao et al.^{11,12} using amphiphilic triblock copolymers to direct the organization of silica species under strong acidic conditions.

SBA-15 has regular, cylindrical, ordered hexagonal pores, with narrow pore size distribution and large surface area. Its pore diameters is larger (2–10 nm) compared to common zeolites, enabling large metallocene molecules to be immobilized not only onto the surface but also inside the pores of the supports. Furthermore, the geometrical shape of the nanochannels can serve as polymerization reactors to affect the pattern of monomer insertion and to control polymer chain structure, polymer chains arrangement, and polymer morphology.^{13,14}

After silica, the most commonly used commercial support is silica–titania. Although titania itself functions poorly as a support for Phillips catalysts, when a few percent titania is added to Cr/silica it serves as a strong promoter for the chromium, increasing its activity and lowering the polymer MW.^{5,15–21}

In our previous reports on the Cr/silica catalysts,^{22,23} the effects of the polymerization temperature and silica structure on the catalytic activities and morphologies of the produced PEs are investigated. Here, we report the synthesis and characterization of aluminum and titanium containing SBA-15 materials and their behavior in ethylene polymerization after chromium incorporation by grafting.

EXPERIMENTAL

Materials

All manipulations involving air and/or water sensitive compounds were performed under nitrogen atmosphere using standard Schlenk technology.

TEAL (triethylaluminum) and Pluronic 123 triblock copolymer (EO₂₀–PO₇₀–EO₂₀) were purchased from Aldrich. Tetraethylorthosilicate (TEOS), tetraisopropyl orthotitanate, aluminum isopropoxide, HCl, and ethanol were obtained from Merck. Polymerization-grade ethylene was purified using three columns of KOH, CuO, and 5 Å molecular sieves. Hexane was refluxed over sodium with benzophenone as an indicator and distilled under nitrogen atmosphere before use.

Preparation of the Supports

Al/SBA-15 material was synthesized according to the procedure described by Yue et al.²⁴ In a typical preparation, 8.6 g of TEOS and given amount of aluminum isopropoxide (Si/Al = 30) was dissolved in 10 mL of HCl solution (pH = 1.3). The mixture was stirred at room temperature for 4 h, then was added to second solution containing 4 g of Pluronic 123 in 150 mL of HCl solution (pH = 1.5). The mixture was stirred at 40°C for 20 h. The mixture was aged at 140°C for 24 h under static conditions. The solid product was filtered off, washed, and air-dried at room temperature overnight. The template was removed from the as-made mesoporous material by calcination at 550°C for 5 h and heating rate 5°C min⁻¹ under pure N₂. An ICP analysis gave the Si/Al = 29.

Ti/SBA-15 supports were synthesized using Pluronic 123 triblock copolymer (EO₂₀–PO₇₀–EO₂₀; Aldrich) as template. In a typical preparation, 4 g of P123 was dissolved in mixture of 30 g of water and 120 g of 2 M HCl solution. Then 8.5 g of TEOS and 0.2 mL tetraisopropyl orthotitanate (Si/Ti = 35) was added into the solution respectively with stirring at 35°C for 20 h. The solid product was recovered, washed, and air-dried at room temperature overnight. The mixture was aged at 80°C for 24 h under static conditions. The template was removed from the as-made mesoporous material by calcinations at 550°C for 6 h and heating rate 5°C min⁻¹ under pure N₂ or soxhlation in ethanol solvent. An ICP analysis gave the Si/Ti = 34.

Preparation of the Silica Supported Catalysts

Chromium grafting procedure started with calcined support materials outgassed under vacuum conditions overnight. Then, 2 g of the sample was stirred with 30 mL of chromium nitrate nonahydrate solution in dried methanol for 3 h under reflux. Next, solids were recovered by filtration and intensively washed with methanol. Finally, grafted materials were oxidized with air on a fluidized bed reactor up to 550°C for 3 h with a heating rate of 2.0°C min⁻¹. ICP analysis gave the supported chromium content (0.19 wt %).

Preparation of Nanopolyethylene in Slurry Phase

Ethylene polymerization reactions were carried out in a 2-L stainless steel stirred autoclave engineers apparatus. Reaction conditions were 800 rpm, 90°C, 31.5 bar of ethylene, 0.5 mol of TEAL using *n*-hexane as solvent. After 1 h of reaction, the resulting polyethylene (PE) was recovered, filtered, washed with

acetone and dried for 6 h at 70°C. Polymerization activities (kgPE gCr⁻¹ h⁻¹) were calculated for each run.

Characterization of Support, Chromium Catalyst, and Polyethylene

Inductively coupled plasma-atomic emission spectroscopy (ICP-AES, 3410, Switzerland) was used to determine the elemental analysis of the synthesized catalysts. First 2.5 mL of concentrated sulfuric acid was added dropwise to the 0.25–0.5 g of sample. Then 25–30 mL of concentrated hydrofluoric acid was added. Then the solvent was evaporated and the remained solid was dissolved in 25 mL water. About 2 mL of concentrated sulfuric acid was added and heated until the white smoke of SO₂ was observed. Then the mixture after cooling to room temperature was added to 5 mL concentrated hydrochloric acid. The solution was heated 5–10 min until clear solution was obtained.

Powder X-ray diffraction (XRD) patterns were collected on a SiemensD5000 diffractometer (Siemens, Berlin, Germany) instrument using Cu K α radiation of wavelength 0.154 nm. Nitrogen adsorption–desorption isotherms was obtained at 77 K using an OMNISORP (TM) 100CX VER 1G adsorption apparatus (USA). Samples were outgassed at 473 K for at least 8 h in vacuum prior to measurements. The supports and polymer samples were deposited on a sample holder and sputtered with gold. The morphologies were observed on a scanning electron microscopy (SIRION, FEI, USA). Transmission electron micrographs (TEM) were taken on a 2000 JEOL electron microscope (Akishima, Japan) operating at 200 kV. The samples for TEM were prepared by dispersing a large number of particles of the products through a slurry in acetone onto a holey carbon film on a Ni grid.

Differential scanning calorimetry (DSC) analysis was carried out on a Perkin-Elmer (Pyris 1, USA) DSC 7 instrument. Ultrahigh purified nitrogen was purged through the calorimeter. The PE samples (\approx 4 mg) were heated to 170°C at a rate of 10°C min⁻¹, they were then cooled to 40°C at 10°C min⁻¹. Subsequently, a second heating cycle was conducted at a heating rate of 10°C min⁻¹.

RESULTS AND DISCUSSION

Characterization of Supports

X-ray diffraction patterns of the calcined mesoporous supports, denoted as SBA-15 (hexagonal), Al/SBA-15 and Ti/SBA-15 are illustrated in Figure 1. All materials exhibit well resolved diffraction peaks that can be indexed as the (100), (110), and (200) reflections associated with P6mm hexagonal symmetry typical of SBA-15 materials.¹¹ These peaks are slightly shifted to lower angle values with aluminum insertion indicating a higher *d*-spacing. This fact is related to the longer Al–O bond length compared to the Si–O bond.^{25,26} So the aluminum incorporation produces a slight expansion of the solid structure.

Similar to Al/SBA-15, these peaks are slightly shifted to lower angle values with titanium insertion indicating a higher *d*-spacing. This change may be attributed to longer Ti–O bond length compared to the Al–O and Si–O bonds. Expansion of the solid structure with titanium incorporation is slightly more than aluminum containing support. Against to SBA-15,

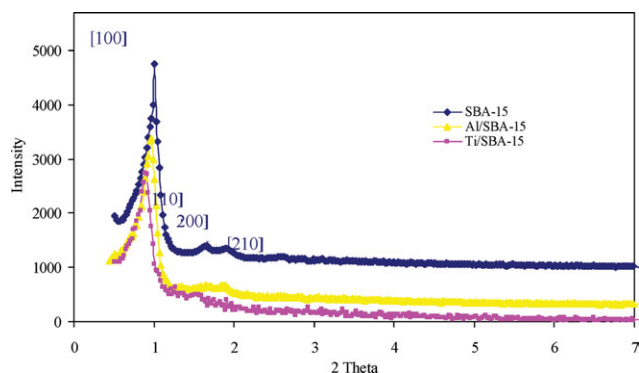


Figure 1. X-ray diffraction pattern of the soxhleted SBA-15 support (◆), Al/SBA-15 (▲) and Ti/SBA-15 (■). [Color figure can be viewed in the online issue, which is available at wileyonlinelibrary.com.]

diffraction peak of (200) was disappeared in Ti/SBA-15 that may be related to destruction of well-ordered structure of Ti/SBA-15 support.

Table I summarizes the textural properties of the supports. It can be observed that BET surface area, pore size, and pore volume increase upon insertion of aluminum^{27,28} and titanium in agreement with the literature. Besides, larger pores detected in Al/SBA-15 and Ti/SBA-15 materials are responsible of the lower wall thickness values as shown in Table I. It is remarkable that important changes in the textural properties are produced when

Table I. Structural Parameters of Supports

Sample	Support	S_{BET} ($m^2 g^{-1}$)	d_p (\AA)	V_p ($mL g^{-1}$)	d_{100} (\AA)	b_p (\AA)
1	SBA-15(Hex)	479	35.8	0.51	87	32.4
2	Al/SBA-15	820	126	1.54	130	12.1
3	Ti/SBA-15	850	132	1.75	135	12.0

S_{BET} , BET specific surface area; V_p , specific pore volume; d_p , average pore diameter, obtained from BJH adsorption data, $d_p = 4V_p/S_{BET}$; d_{100} , XRD interplanar spacing; b_p , pore wall thickness, $b_p = (a_0 - d_p)/2$, $a_0 = (2/\sqrt{3})d_{100}$.

a low amount of aluminum and titanium is incorporated into SBA-15 material.

TEM images [Figure 2(b, c)] confirm that Al/SBA-15 and Ti/SBA-15 have a two-dimensional $p6mm$ hexagonal structure, with a well ordered hexagonal array and one-dimensional channel structure that is characteristic properties of SBA-15. The average distance between mesopores is about 115–130 \AA , in agreement with that determined from the N_2 adsorption isotherms.

Scanning electron microscopy was also used to determine the size and morphology of the synthesized supports. In Figure 3(b) SEM micrographs show that the Al/SBA-15 particles have tubular structure with 1–2 μm long and 0.2–0.3 μm in diameters, and each particle consists of many hexagonal nanochannels.

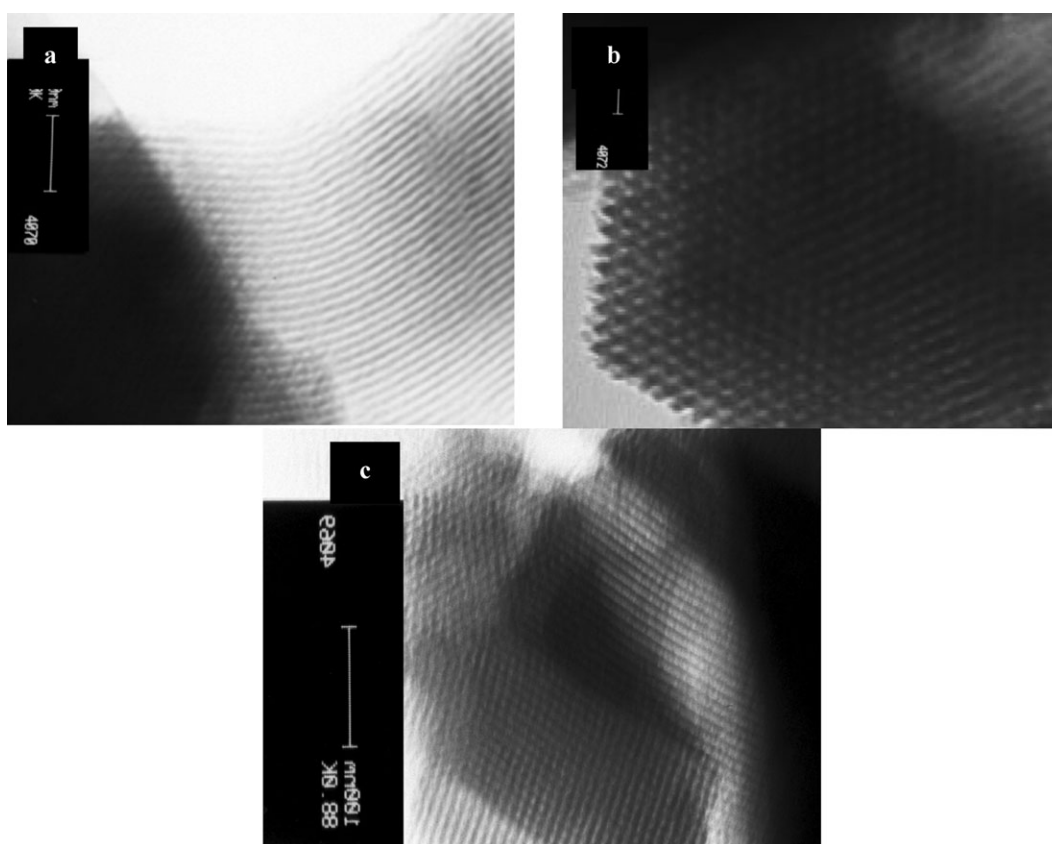


Figure 2. TEM micrographs of (a) SBA-15, (b) Al/SBA-15, and (c) Ti/SBA-15.

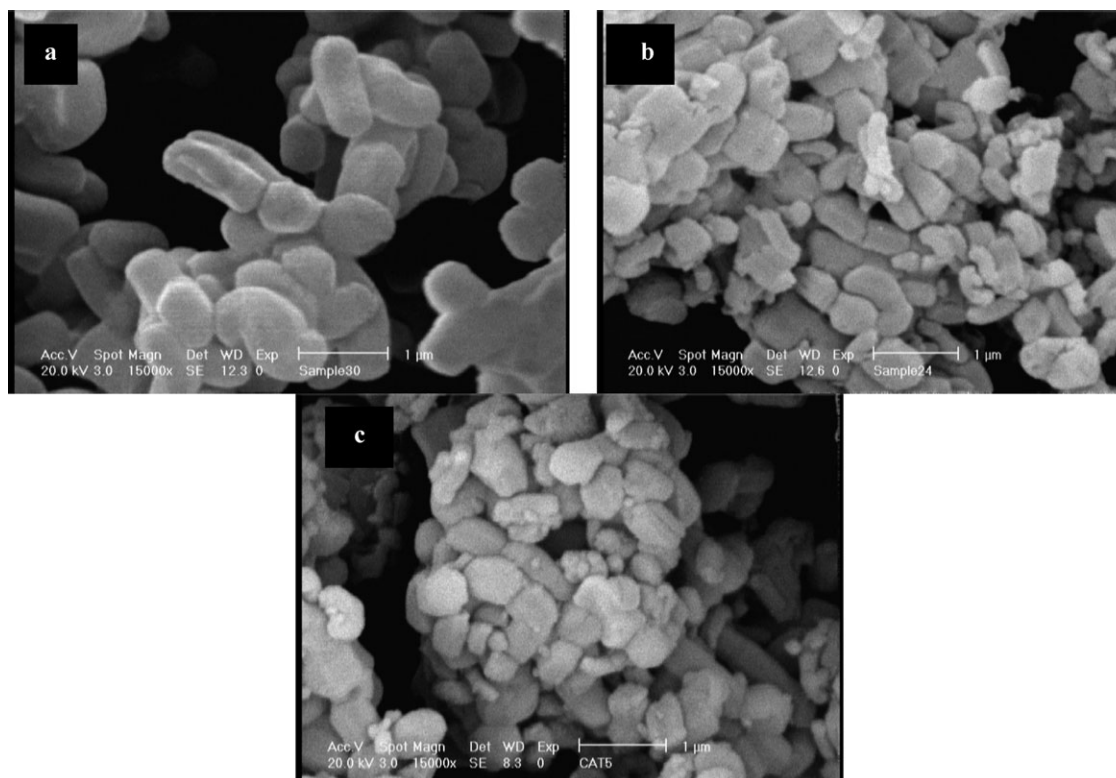


Figure 3. SEM micrographs of (a) SBA-15, (b) Al/SBA-15, and (c) Ti/SBA-15.

Figure 3(c) shows that the Ti/SBA-15 particles have tubular structure with 0.5–1 μm long and 0.2–0.5 μm in diameters.

Ethylene Polymerization Results

The influence of the different parameters such as chromium content and support on the catalytic activity of Cr/SBA-15 was investigated to obtain the highest polymerization activity. For the Cr/SBA-15 catalysts, the chromium loading was varied from 0.1 to 1 wt % (Figure 4). The results indicate a first-order tendency to zero-order dependence at higher chromium content. The initial rates of reaction, in the absence of external mass transfer resistance, are plotted against catalyst loading in Figure 4. It demonstrates that the rates are directly proportional to catalyst loading, due to proportional increase in the number of active sites. Increasing of the chromium content >0.2 wt % has practically no effect on the polymerization rate. Metal catalyzed mass transfer reaction was defined by zero-order dependence of catalytic activity and metal concentration.^{29,30} According to the Wiesz–Prater criterion, the results were analyzed to assess the influence of the pore diffusion resistance and mass transfer as rate-controlling factors.³⁰ The zero-order dependence of Cr(VI)/SBA-15 catalyst to activity only related to the intrinsic reaction rate rather than mass transfer control. All catalysts were tested under the optimized reaction condition.

Table II presents the ethylene polymerization activities of Cr/SBA-15 catalysts compared to Cr/Ti/SBA-15 and Cr/Al/SBA-15 as well as the main properties of the resulting polymers: activity, melt temperature, crystallinity and bulk density.

The activity of Cr/Ti/SBA-15 is 845 kgPE $\text{gCr}^{-1} \text{h}^{-1}$ that is the highest value among other catalysts. It is remarkable that the very low catalytic activity showed by Cr/SBA-15 sample in spite of the high surface area of SBA-15. The probable explanation is that the polymer just formed immediately fills up the pores of the material and, at the same time, since the catalyst structure is not fragile enough, it does not fragment into smaller pieces. So that the material cannot produce further polymer and no subsequent activity is observed. Fragility is often correlated with pore volume. Thus, Cr/silica catalysts containing much $<1.0 \text{ cm}^3 \text{ g}^{-1}$ pore volume and 100 \AA pore size, usually do not exhibit polymerization activity.^{2,31} In this way, small pore size,

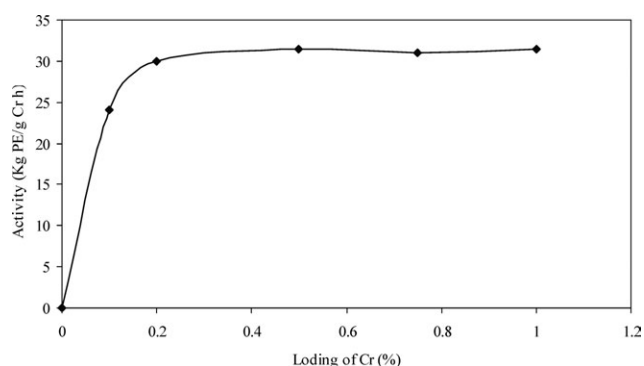


Figure 4. Effect of chromium content on the activity of Cr/SBA-15 (cocatalyst = triethyl aluminum (TEAL), solvent = *n*-hexane, polymerization temperature = 104°C, ethylene pressure = 31.5 bar).

Table II. Ethylene Polymerization Results with Different Chromium Supported Catalysts

Run ^a	Catalysts	Activity ^b	Bulk density (g mL ⁻¹)	T_m (°C) ^c		ΔH (J g ⁻¹)		Crystallinity ^d
				First scan	Second scan	First scan	Second scan	
1	Cr/SBA-15(Hex)	34	0.19	142.6	138.0	224.1	182.5	76.3
2	Cr/Al/SBA-15	612	0.28	143.5	135.2	194.5	132.5	66.3
3	Cr/Ti/SBA-15	845	0.29	139.6	134.4	145.6	97.8	49.6

^aEthylene pressure = 31.5 bar; solvent = *n*-hexane; cocatalyst = TEAL, T_p (polymerization temperature) = 90°C. ^bkg PE⁻¹ g⁻¹ Cr⁻¹ h⁻¹. ^cMelting temperature measured by DSC. ^dCrystallinity measured by XRD.

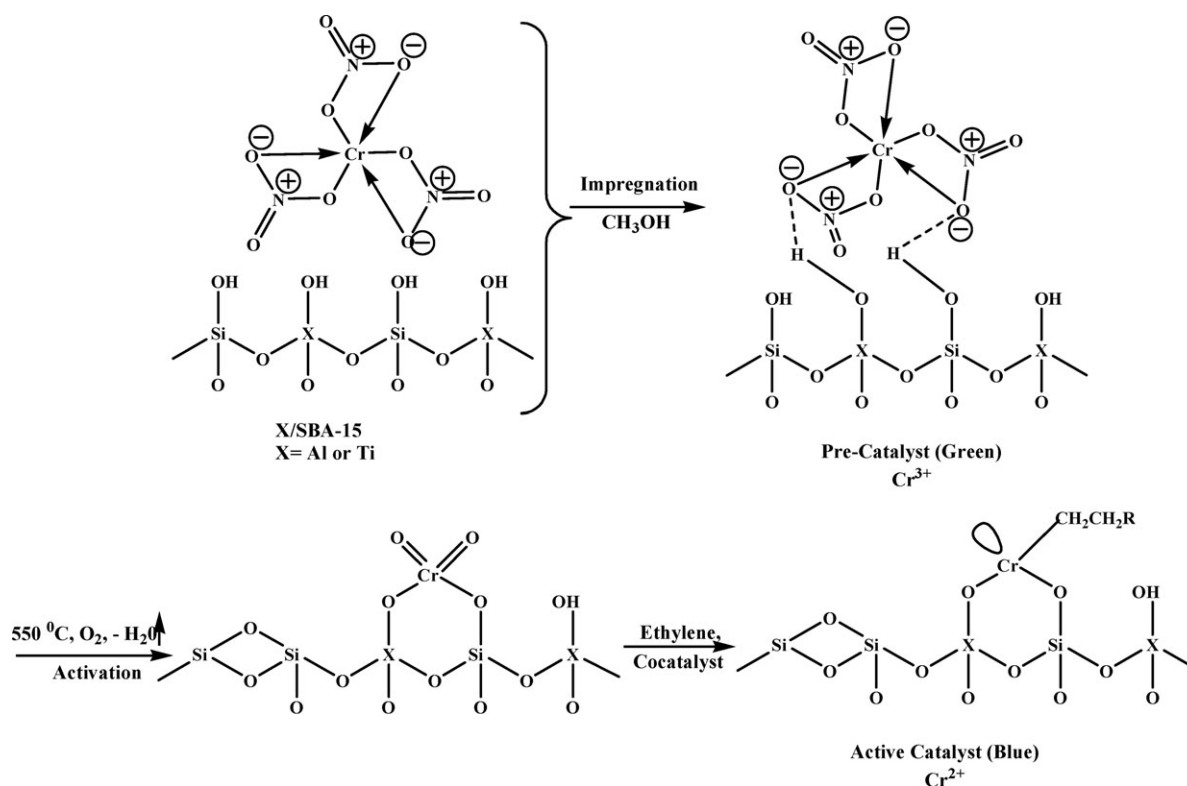
small pore volume and high wall thickness of SBA-15 support (Table I) are responsible for the low polymerization activity exhibited by Cr/SBA-15 catalyst compared to other catalysts.

Therefore, it would be necessary to increase both pore size and volume of siliceous SBA-15 mesoporous material to get a suitable support to prepare Phillips type catalysts useful for ethylene polymerization. A possible way to do it is to use a swelling agent during the synthesis step. This approach has been already explored³² using trimethylbenzene in the synthesis of siliceous SBA-15 mesoporous materials to prepare Cr/SBA-15 catalysts with better catalytic activities than conventional Cr/SiO₂.

One method to increase the pore size and volume of SBA-15 mesoporous material and activity of Cr/silica catalyst is using additives such as Ti, Al, Zr, Mo, etc. In this article, the effect of aluminum and titanium incorporation on the polymerization

activity has been evaluated. After silica, the most commonly used commercial support is silica–titania. Although titania itself functions poorly as a support for Phillips catalysts, when a few percent titania is added to Cr/silica it serves as a strong promoter for the chromium, increasing its activity (Table II). The addition of titania to silica enhances the Brønsted acidity of the surface, and the chromium may become associated with or linked to these now strongly acidic Brønsted sites. This bonding would tend to make the chromium more electron deficient, and therefore possibly more reactive with olefins.^{33,34} The increase in surface acidity may derive from an ability of Ti(IV) to assume a tetrahedral coordination and fit in with the silica lattice.³⁵

Table II also shows that Cr/Al/SBA-15 catalyst displays a high catalytic activity. Perhaps the most well-known method of



Scheme 1. Mechanism of polymerization using different chromium supported catalysts.

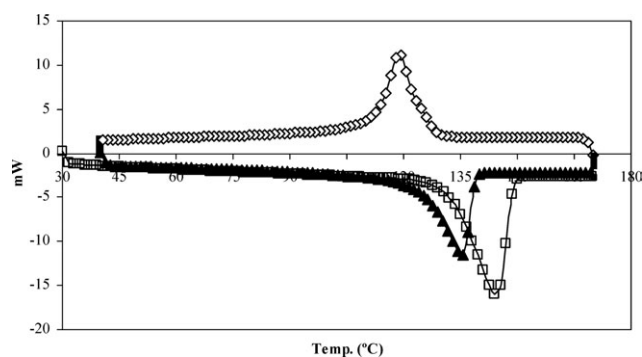


Figure 5. DSC thermograms of polyethylene produced by Cr/Al/SBA-15. Heating rate $20^{\circ}\text{C min}^{-1}$ under pure N_2 . (\square) Run1 (40–170°C) $20^{\circ}\text{C min}^{-1}$ under pure N_2 , (\diamond) Run2 (170–40°C) $-20^{\circ}\text{C min}^{-1}$ under pure N_2 , and (\blacktriangle) Run3 (40–170°C) $20^{\circ}\text{C min}^{-1}$ under pure N_2 .

increasing the acidity of silica is to add alumina.¹⁵ It is clear that the polymerization activity of Cr/Al/SBA-15 catalyst is significantly improved by aluminum insertion to the support. The result of adding alumina is much like that obtained by adding titania.

As noted earlier, these effects are perhaps caused by Cr(VI) ions attached to Brönsted acid sites, which possibly pull electron density away from the chromium, making it more Lewis acidic. This change in electron density could favor the agnostic β -hydride coordination that is a precursor for chain termination and transfer. Notwithstanding the similar results observed after the addition of alumina and titania to the silica surface, the effect of titania is the stronger, perhaps because of greater thermal stability.^{36–38} The earliest Phillips catalysts used silica–alumina as a support rather than just silica, and Cr/silica–alumina is still used today for certain blow molding applications.

These facts could be explained taking into account that wall thickness of Ti/SBA-15 and Al/SBA-15 samples are reduced by Ti or Al incorporation resulting at the same time in higher pore volumes (Table I). High pore volume, pore size, and small wall thickness of modified supports are responsible for high polymerization activity of polymer exhibited by the Cr/Al/SBA-15 and Cr/Ti/SBA-15 catalysts. These two circumstances lead to materials that are more fragile and consequently more active in ethylene polymerization.

As shown in Scheme 1 Cr/Al/SBA-15 and Cr/Ti/SBA-15 catalysts have been prepared using impregnation method. Chromium nitrate (III) nonahydrate was coordinated to the silica surface. Hydrogen bonding between OH group at the silica surface and nitrate ligand is shown schematically. Cr(III) was pseudooctahedrally coordinated to the silica surface. After calcination Cr(III) was completely changed to Cr(VI) while most of them in dichromate state, some of them in chromate state and little amount of them in amorphous cluster of Cr_2O_3 and cubic pyramidal Cr(V) were bonded to silica surface.^{39,40}

As shown in the Scheme 1, the addition of titania creates a new population of more easily reducible sites. The addition of titania to silica enhances the Brönsted acidity of the surface, and the chromium may become associated with or linked to these now

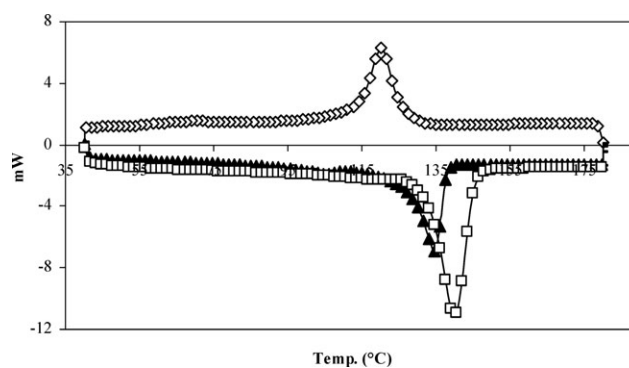


Figure 6. DSC thermograms of polyethylene produced by Cr/Ti/SBA-15. Heating rate $20^{\circ}\text{C min}^{-1}$ under pure N_2 . (\square) Run1 (40–180°C) $20^{\circ}\text{C min}^{-1}$ under pure N_2 , (\diamond) Run2 (180–40°C) $-20^{\circ}\text{C min}^{-1}$ under pure N_2 , and (\blacktriangle) Run3 (40–180°C) $20^{\circ}\text{C min}^{-1}$ under pure N_2 .

strongly acidic Brönsted sites. This bonding would tend to make the chromium more electron deficient, and therefore possibly more reactive with olefins.^{33,34}

Other data also suggest that Cr(VI) may be less stable when associated with titania.^{41–43} So the overall activity was raised and increased by titania in two ways: first, by shortening the induction time, bringing sites to life more quickly, and second, by raising the polymerization rate itself. These results confirm that titania creates a unique Cr(VI) species that is more easily reduced. The increased polymerization rate is probably the result of this new population of sites, although it is not certain whether the total active-site concentration is increased by titania. A small amount of titania significantly improves activity, but the effect wanes at high loadings. At very high loadings some activity may even be lost, as pores begin to clog.

The DSC results in Table II show that the melting point of the polymer prepared from Cr/Al/SBA-15 catalyst (143.5°C) is higher than Cr/Ti/SBA-15 catalyst (139.6°C) and similar to Cr/SBA-15 catalyst (142.6°C). In Figure 5 DSC curve of polyethylene prepared from Cr/Al/SBA-15 is shown. In second scan, recrystallization significantly decrease the melting point that is may be related to degradation of polyethylene nanofiber. According to Table II the high melting point of the polymer prepared from Cr/SBA-15 (142.6°C) compared with HDPE may

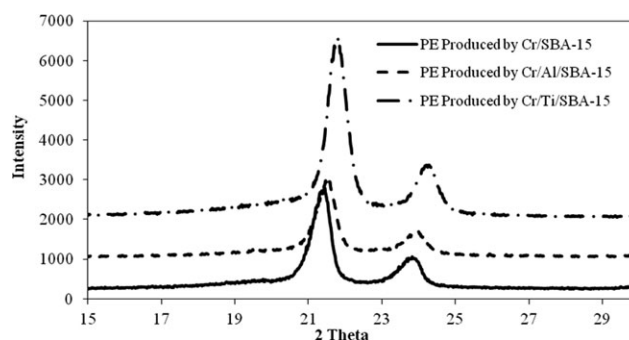


Figure 7. X-ray diffraction pattern of the polyethylene produced by Cr/SBA-15 (—), Cr/Al/SBA-15 (---), and Cr/Ti/SBA-15 (-·-).

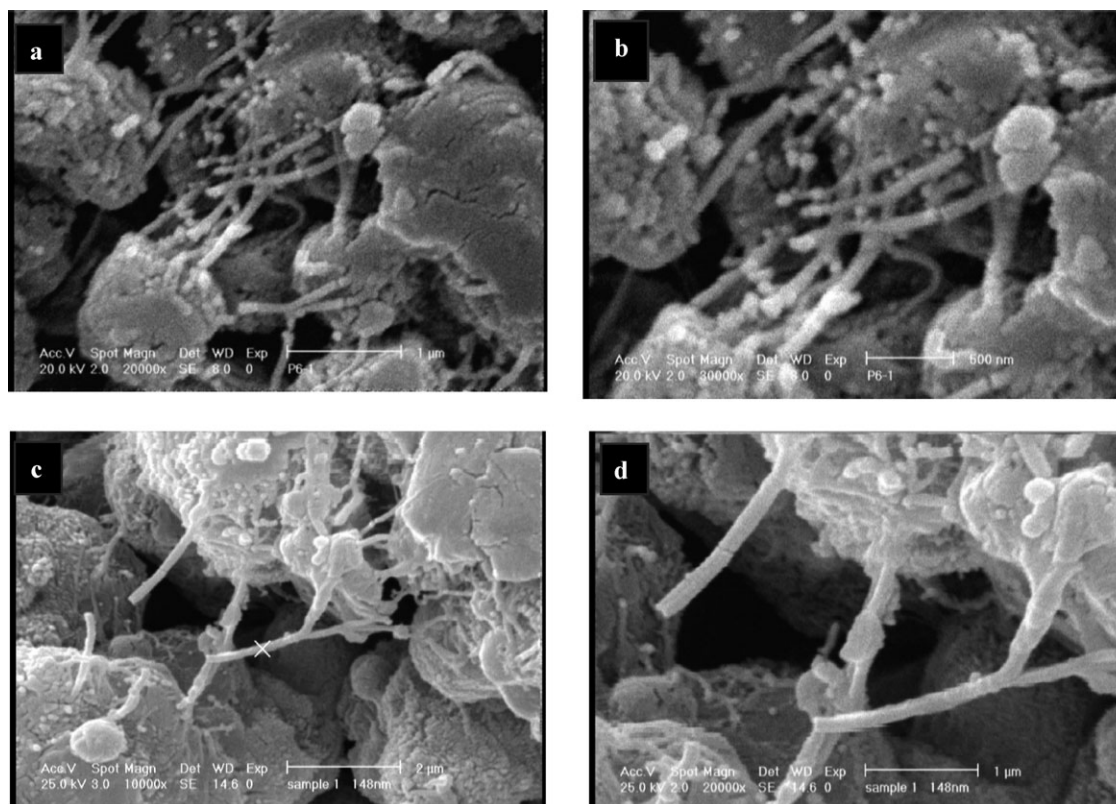


Figure 8. SEM micrographs of the polyethylene produced from chromium supported catalysts at 90°C (a) Cr/Al/SBA-15 (b) magnified view of (a), (c) Cr/Ti/SBA-15 (d) magnified view of (c).

be related to the high molecular weight, long chains having a small number of side branches and nanofiber formation. As shown in Figure 6 weak peak observed around 104.5°C is related to the melting point of low molecular weight polyethylene.

Figure 7 shows the XRD spectra of the PE prepared by silica-supported catalysts. The typical [110] and [200] diffraction peaks at 21.5° and 24.0°, respectively, testify the orthorhombic crystalline structure. There also is a small amorphous halo around 19.50°, indicating the existence of amorphous polyethylene. The results show that polyethylene prepared from Cr/SBA-15(Hex) catalyst has higher crystallinity among other polyethylene because the channels of SBA-15 can control the direction of the chain propagation to increase the crystallinity of the polyethylene.

In polymers produced by Cr/Al/SBA-15 and Cr/Ti/SBA-15 change in diffraction peaks toward higher 2-theta shows that *d*-spacing of PE prepared from modified catalysts are lower than PE prepared from Cr/SBA-15. This change may be attributed to structural changes in catalyst and support order decrease that is shown in Figure 3.

Figure 8 shows the SEM micrographs of the sample produced in Table II run 2 and 3, these indicates that the PE samples mainly take on porous morphologies and partially nanofiber morphology. So the morphology also confirms the lower crystallinity of Al/Cr/SBA-15 and Ti/Cr/SBA-15.

CONCLUSIONS

Ethylene polymerization catalysts have been prepared by grafting chromium (III) nitrate onto SBA-15 mesoporous materials. BET surface area, pore size and pore volume of SBA-15 supports increase upon insertion of aluminum and titanium, while the wall thickness is reduced. Al and Ti incorporation favors chromium anchorage onto SBA-15 surface. Small pore size (35.8 Å), pore volume (0.51 cm³ g⁻¹) and high wall thickness (32.4 Å) of siliceous SBA-15 support are responsible for lower polymerization activity exhibited by the Cr/SBA-15 catalyst. On the other hand, the polymerization activity of Cr/Ti/SBA-15 catalysts is significantly improved by titanium insertion to the supports. Titania and alumina with increasing the acid strength of a support usually improves the activity of the catalyst. Thus, the acidic silica–titania or silica–alumina is typically more active than silica. Particularly, catalyst prepared with Al/SBA-15 support is almost four times more active than a conventional Cr/SiO₂ Phillips catalyst. Polymers obtained with all of the catalysts showed melting temperature, bulk density and high load melt index indicating the formation of linear high-density polyethylene.

ACKNOWLEDGMENTS

Dr Ebrahim Ahmadi made a substantial contribution to the research design; Dr Zahra Mohamadnia participated in revising the article; Asemeh Mashhadi-Malekzadeh and Fatemeh Saghatchi

performed the experiments; Zahra Hamdi analyzed the synthetic materials and interpreted the data.

REFERENCES

1. Fawcett, E. W.; Gibson, R. O.; Perrin, M. W.; Patton, J. G.; Williams, E. G. *Brit. Pat.* 472,590, **1937**.
2. McDaniel, M. P. In *Handbook of Heterogeneous Catalysis*; Ertl, G., Knözinger, H., Weitkamp, J., Eds.; VCH-Wiley: Weinheim, Germany, **1997**; Vol. 5, p 2400.
3. Clark, A.; Hogan, J. P.; Banks, R. L.; Lanning, W. C. *Ind. Eng. Chem.* **1965**, 48, 1152.
4. Clark, A. *Adv. Chem. Ser.* **1969**, 91, 387.
5. McDaniel, M. P. *Adv. Catal.* **1985**, 33, 47.
6. Weckhuysen, B. M.; Schoonheydt, R. A. *Catal. Today* **1999**, 51, 215.
7. Scott, S. L.; Amor NaitAjjou, J. *Chem. Eng. Sci.* **2001**, 56, 4155.
8. Ertl, G.; Knozinger, H.; Weitkamp, J., Eds. *Handbook of Heterogeneous Catalysis*; VCH: Verlagschaft, **1997**; Vol. 5, p 2400.
9. Groppo, E.; Lamberti, C.; Bordiga, S.; Spoto, G.; Zecchina, A. *Chem. Rev.* **2005**, 105, 115.
10. Groppo, E.; Lamberti, C.; Spoto, G.; Bordiga, S.; Magnacca, G.; Zecchina, A. *J. Catal.* **2005**, 236, 233.
11. Zhao, D.; Feng, J.; Huo, Q.; Melosh, N.; Fredrickson, G. H.; Chmelka, B. F.; Stucky, G. D. *Science* **1998**, 279, 548.
12. Zhao, D.; Huo, Q.; Feng, J.; Chmelka, B. F.; Stucky, G. D. *J. Am. Chem. Soc.* **1998**, 120, 6024.
13. Dong, X.; Wang, L.; Jiang, G.; Zhao, Z.; Sun, T.; Yu, H.; Wang, W. *J. Mol. Catal. A Chem.* **2005**, 240, 239.
14. Kresge, C. T.; Leonowicz, M. E.; Roth, W. J.; Vartuli, J. C.; Beck, J. S. *Nature* **1992**, 359, 710.
15. Horvath, B. US Pat. 3,625,864, **1971**.
16. McDaniel, M. P.; Welch, M. B.; Dreiling, M. J. *J. Catal.* **1983**, 82, 118.
17. Pullukat, T. J.; Hoff, R. E.; Shida, M. *J. Polym. Sci. Polym. Chem. Ed.* **1980**, 18, 2857.
18. Conway, S. J.; Falcone, J. W.; Rochester, C. H.; Downs, G. W. *J. Chem. Soc. Faraday Trans. 1* **1989**, 85, 1841.
19. Bouh, A. O.; Rice, G. L.; Scott, S. L. *J. Am. Chem. Soc.* **1999**, 121, 7201.
20. Deitz, R. E. US Pat. 3,887,494, **1975**.
21. Rebenstorf, B.; Sheng, T. C. *Langmuir* **1991**, 7, 2160.
22. Ahmadi, E.; NekoomaneshHaghighi, M.; Mohamadnia, Z.; Ramazani, A. *J. Appl. Polym. Sci.* **2010**, 118, 3658.
23. Mohamadnia, Z.; Ahmadi, E.; Nekoomanesh, M.; Ramazani, A.; Salehi-Mobarakeh, H. *Polym. Int.* **2010**, 59, 945.
24. Yue, Y.; Gédéon, A.; Bonardet, J. L.; Melosh, N.; D'Espinose, J. B.; Fraissard, J. *Chem. Commun.* **1999**, 1967.
25. Legrand, A. P., Ed. *The Surface Properties of Silicas*; Wiley: **1997**; p 2.
26. Sklad, P. S.; Angelini, P.; Sevely, J. *Phil. Mag. A* **1992**, 64, 1445.
27. Yue, Y. H.; Gédéon, A.; Bonardet, J. L.; d'Espinose, J. B.; Melosh, N.; Fraissard, J. *Stud. Surf. Sci. Catal.* **2000**, 129, 209.
28. Springuel-Huet, M. A.; Bonardet, J. L.; Gédéon, A.; Yue, Y.; Romannikov, V. N.; Fraissard, J. *Micropor. Mesopor. Mater.* **2001**, 44, 775.
29. Satterfield, C. N. *Mass Transfer in Heterogeneous Catalysis*; Krieger: New York, **1970**; p 164.
30. Fromet, G. F.; Bischoff, K. B. *Chemical Reactor Analysis and Design*; Wiley: New York, **1979**; p 191.
31. McDaniel, M. P.; Witt, D. R.; Benham, E. A. *J. Catal.* **1998**, 176, 344.
32. Calleja, G.; Aguado, J.; Carrero, A.; Moreno, J. *Stud. Surf. Sci. Catal. B* **2005**, 158, 1453.
33. Ellison, A.; Overton, T. L. *J. Mol. Catal.* **1994**, 90, 81.
34. Ellison, A.; Overton, T. L. *J. Chem. Soc. Faraday Trans.* **1993**, 89, 4393.
35. Soult, A. S.; Carter, D. F.; Schreiber, H. D.; Van de Burgt, L. J.; Stiegman, A. E. *J. Phys. Chem. B* **2002**, 106, 9266.
36. Schreiber, L. B.; Vaughn, R. W. *J. Catal.* **1975**, 40, 226.
37. Clark, A. *Catal. Rev.* **1969**, 3, 145.
38. Rebenstorf, B.; Lars, S.; Anderson, T. *J. Chem. Soc. Faraday Trans.* **1990**, 86, 3153.
39. Calleja, G.; Aguado, J.; Carrero, A.; Moreno, J. *Catal. Commun.* **2005**, 6, 153.
40. Calleja, G.; Aguado, J.; Carrero, A.; Moreno, J. *Appl. Catal. A Gen.* **2007**, 316, 22.
41. Weckhuysen, B. M.; Wachs, I. E.; Schoonheydt, R. A. *Studies in Surface Science and Catalysis: Preparation of Catalysts VI*; Elsevier: Amsterdam, **1995**; Vol. 91, p 151.
42. Hardcastle, F. D.; Wachs, I. E. *J. Mol. Catal.* **1988**, 46, 173.
43. McDaniel, M. P. *Adv. Catal.* **2010**, 53, 123.